

## Study of the Influence of a Mixed Electrolyte of Oxalic Acid and DBSA on the Properties of Co-Deposited Poly(Aniline-Co-Pyrrole)

R.A. Flores-Estrella<sup>1,2</sup>, D.E. Pacheco<sup>1</sup>, M.J. Aguilar Vega<sup>1</sup> and Mascha A. Smit<sup>1,\*</sup>

<sup>1</sup> Unidad de Materiales, Centro de Investigación Científica de Yucatán (CICY), Calle 43 no. 130 Chuburná de Hidalgo, 97200, Mérida, Yucatán, México

<sup>2</sup> Facultad de Ingeniería Química, Universidad Autónoma de Yucatán, Mérida, Yucatán, México

\*E-mail: [mascha@cicy.mx](mailto:mascha@cicy.mx)

Received: 23 May 2008 / Accepted: 15 June 2008 / Published: 4 August 2008

---

Aniline and pyrrole copolymers were synthesized for different monomer ratios from a mixed electrolyte containing 0.1M oxalic acid and 0.1M dodecyl benzene sulphonic acid (DBSA) using a 4-step electrochemical method. Results were compared to those obtained for polymers prepared from an electrolyte of oxalic acid only. It was found that the presence of DBSA increases the polymerization rates for polymer deposited from the mixed monomer electrolytes, but not for the homopolymers. For copolymers deposited from monomer mixtures of high aniline content, deposition rates were generally low, due to the low conductivity of these samples. FTIR and cyclic voltammetry results confirm the presence of both monomers in the polymers deposited from the mixed electrolyte, and FTIR indicates that copolymers, rather than mixtures, are formed. Results from AC impedance spectroscopy show that the presence of DBSA results in an increased double layer capacitance for the homopolymers and increased low frequency capacitance for those samples with low pyrrole content.

---

**Keywords:** Copolymers, electropolymerization, polypyrrole, polyaniline, cyclic voltammetry, electroconductive polymers

### 1. INTRODUCTION

Due to their unique combination of properties, intrinsically electroconductive polymers have a wide range of applications, from coatings, electronic devices, LED's, sensors, batteries, to solar cells and many more. In recent years, interest has increased for applications in fuel cells, for example as catalyst support material [1,2], and more recently as catalyst material [3], and applications in supercapacitores [4,5], in which case advantage is taken of the so-called pseudocapacitance obtained from Faradaic processes. Since the specific properties of the conductive polymers, such as conductivity

and electroactivity, depend on the specific polymer and the specific production method, it is of great interest to study how to obtain desired characteristics for these specific applications. Though several highly conductive and relatively stable polymers, such as polypyrrole, polyaniline and polythiophene, are well known and have been thoroughly studied, new combinations of properties can be obtained by the preparation of copolymers.

Copolymers have been prepared from monomers with similar chemical structure, such as aniline with substituted anilines like 2-methylaniline and 2-ethylaniline [6,7] and also from monomers having the same aromatic structure, such as pyrrole and thiophenes [8]. Since polyaniline and polypyrrole are some of the more common intrinsically electroconductive polymers, the preparation of poly(aniline-co-pyrrole) is a logical step. However, these monomers have a different aromatic structure.

The structure and properties of copolymers based on aniline and pyrrole prepared by electrochemical methods were reported to depend significantly on the solvent and supporting electrolyte [9]. Fusalba and Belanger [10] copolymerized aniline and pyrrole galvanostatically in an organic acidic medium and obtained a mixture of homopolymer and random copolymer. Iroh et al. [11,12] studied the formation of polyaniline-polypyrrole composites on carbon fibres, using a one-step potentiostatic method, as well as on low carbon steel from an oxalic acid solution. Copolymers prepared by oxidative chemical synthesis were reported to have lower conductivity than the corresponding homopolymers, or even are non-conducting [13,14], being an indication that the typical electronic backbone structure of alternated single and double bonds, responsible for the conductivity, was disrupted.

The addition of functionalized protonic acids, such as camphor sulphonic acid (CSA) and dodecyl benzene sulphonic acid (DBSA) to the polymer, leads to superior homogeneity of the polymer films and improves the processability and solubility [15] as well as the dispersion of conductive polymer particles in resins [16]. The effect of a mixed electrolyte containing both small and large dopant ions on the properties of aniline-pyrrole copolymers is not known.

Since the electroconductive copolymers generally have poor mechanical and electrical properties, the aim of this work is to study, whether the co-deposition from a mixed electrolyte may result in better mechanical and electrical properties, with possible applications in supercapacitores, fuel cells and polymer actuators. Therefore, in this study we report on the co-deposition of electroconductive poly(aniline-co-pyrrole) obtained from a mixed electrolyte of oxalic acid and DBSA, and we evaluate the effect on the morphology and on electrochemical and electronic properties of the copolymers in oxalic acid.

## 2. EXPERIMENTAL PART

### 2.1. Electropolymerization

Aniline, (99%), pyrrole (99%, refrigerated), dihydrated oxalic acid (99%) and dodecyl benzene sulphonic acid (99%), were obtained from Sigma-Aldrich. The polymers and copolymers were produced by potentiodynamic electropolymerization. Platinum electrodes with a 0.5 cm diameter were

used as a substrate and the auxiliary electrode was platinum wire. All potentials were measured versus SCE.

The electrolyte was an aqueous solution of 0.1 M oxalic acid ( $\text{H}_2\text{C}_2\text{O}_4$ ) with 0.1 M dodecyl benzene sulphonic acid (DBSA). The total monomer concentration for polymers and copolymers was 0.1 M, in the following ratios of aniline to pyrrole: 100%; 75/25%; 50/50%; 25/75% and 100%. All results were compared to samples prepared under the same conditions without DBSA.

The potentiodynamic polymerization was performed in 4 steps using a Gill AC Autotafel potentiostat: from 0 to 500 mV<sub>SCE</sub> at 500 mV/min; from 500 to 900 mV<sub>SCE</sub> at 60 mV/min; 900 mV<sub>SCE</sub> during 10 min; and potential cycling between 900 and 600 mV<sub>SCE</sub> at 300 mV/min for 10 cycles. To avoid formation of benzoquinone, the lower limit for the potential cycling step was set above 0.5 V. The curves obtained during the 4 different steps of polymerization were converted into one plot of current versus time. Samples were rinsed in methanol after polymerization and dried at 60 °C. The obtained samples were stored in a desiccator.

## 2.2. Characterization

Fourier-transform infrared spectroscopy, FTIR, was performed on a Nicolet Protégé 460 on discs of 1% polymer mixed with KBr. Spectra were recorded between 400 and 4000  $\text{cm}^{-1}$ . Cyclic voltammetry and AC impedance spectroscopy (EIS) were performed in an electrolyte of 0.1 M oxalic acid, using a Gill AC potentiostat, an SCE reference electrode, and a platinum counter electrode. The scan rate for cyclic voltammetry was 50 mV/s. The electrochemical impedance spectroscopy (EIS) was performed in a frequency range between 0.1 Hz to 10 kHz, with a signal amplitude of 10 mV around the open circuit potential. Spectra were recorded hourly during 24 hours. The software Equivalent Circuit (Boukamp) was used to analyze the spectra. Scanning Electron Microscopy (SEM) was performed on a Philips XL30 ESEM.

## 3. RESULTS AND DISCUSSION

### 3.1. Polymerization Curves

Results for the polymerization from an electrolyte containing 50% aniline and 50% pyrrole monomer with and without the presence of DBSA (samples 50A50Ps and 50A50P, respectively), are shown in figure 1. In the first polymerization step current densities are very small. In the second polymerization step, current densities increase up to 3  $\text{mA}/\text{cm}^2$  for both samples, reaching a maximum at potentials around 800 mV. During the third step (constant potential) the currents decrease for samples without DBSA, while for DBSA-containing samples they remain relatively stable. In the last step (potential cycling) current densities for copolymer prepared with DBSA are higher than for those prepared without DBSA, while for the homopolymers the current densities are highest for those without DBSA. The reduced polymerization rates for copolymers obtained from monomer mixtures with higher aniline ratio is related to the reduced electronic conductivity of these samples, caused by

it's different electronic structure obtained for different monomer ratios. This limits charge transfer and so reduces the polymerization rate [13,14].

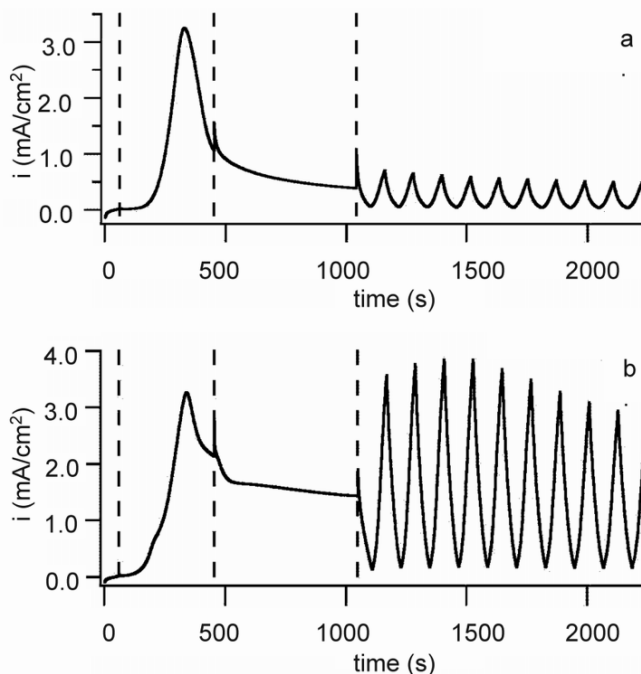


**Figure 1.** Current-time curves for all polymerization steps for polymer prepared from 50% aniline and 50% pyrrole (a.) without DBSA, 50A50P and (b.) with DBSA, 50A50Ps.

Data obtained from the polymerization is shown in table 1. The observed maximum current densities (during the second polymerization step), take place at increasing potentials for increasing pyrrole concentration. For polymers prepared from the same monomer ratio, the maximum was found to be of the same order, as can be seen clearly for the samples with 25%, 50% and 75% pyrrole. It was related to high reaction rates for the oxidation of monomers and of lower oligomers (generation of dications) in this potential range [18]. The current densities found for polypyrrole (100P and 100Ps), were up to 10 times higher than for the polyaniline (100A and 100As), independent of the electrolyte composition, confirming a preference for polypyrrole formation and deposition [11] for the applied 4-step method in these electrolytes.

Based on these curves, the charge transferred during polymerization was calculated for each step, taking the average of 4 samples, see table 1. For all copolymers, the charge transferred during steps 2, 3 and 4 are higher for samples with DBSA, while for polyaniline with DBSA the charge passed in each step is lower, as for polypyrrole with DBSA in steps 2 and 3. The total charge was found to be highest for the homopolymers without DBSA and for the copolymers with DBSA.

Assuming 100% efficiency for the monomer oxidation reaction and polymer deposition onto the substrate, the total charge passed is directly related to the amount of reacted monomer and the mass

of the deposited polymer can be calculated. Results are shown in table 1 and show that for the polymers without DBSA both charge and polymer mass increase in the order of: 75A25P < 50A50P < 25A75P < 100A < 100P, while for samples with DBSA the obtained order was: 100As < 75A25Ps < 50A50Ps < 25A75Ps < 100Ps.

**Table 1.** Sample parameters: composition, maximum current densities (in second polymerization step), charge transferred during polymerization (average from 4 samples), and calculated deposited mass.

sample	composition (mol%)			$i_{\max}$ (mA/cm <sup>2</sup> )	charge transferred (mC)				total charge (C)	mass (mg)
	aniline	pyrrole	DBSA		step 1	step 2	step 3	step 4		
<b>100A</b>	100	0	no	3.9	0.02	271	834	1437	2.54	1.23
<b>75A25P</b>	75	25	no	0.68	0.72	114	126	90	0.331	0.149
<b>50A50P</b>	50	50	no	3.2	0.27	477	398	323	1.2	0.498
<b>25A75P</b>	25	75	no	7.8	0.11	1146	691	571	2.41	0.92
<b>100P</b>	0	100	no	38	2.6	4650	10297	8778	23.7	8.26
<b>100As</b>	100	0	yes	1.2	0.72	148	371	538	1.06	0.511
<b>75A25Ps</b>	75	25	yes	0.78	0.08	171	434	533	1.14	0.512
<b>50A50Ps</b>	50	50	yes	3.2	2.26	592	903	1734	3.23	1.34
<b>25A75Ps</b>	25	75	yes	6.8	2.18	1247	2234	4685	8.17	3.12
<b>100Ps</b>	0	100	yes	13	0.91	2401	5858	8155	16.4	5.71

### 3.2. FTIR spectroscopy

Results obtained from FTIR spectroscopy are shown in figure 2 and 3. No results are shown for samples of 75A25P and 75A25Ps, due to the low amount of polymer formed.

For the polyaniline homopolymer (100A, figure 2) typical bands are shown at 1165, 1010, 830 cm<sup>-1</sup> (C-H), 1380, 1300 and 1250 cm<sup>-1</sup> (C-N), 1597 and 1501 cm<sup>-1</sup> (C-C, quinoid and benzenoid respectively) [19,20,21,22]. The quinoid form, representing the oxidized polyaniline, and the benzenoid, representing the reduced form, appear with similar band intensity, indicating the polymer is in its semi-oxidized form, polyemeraldine. The band at 1730 cm<sup>-1</sup> corresponding to oxalic acid, was not detected, as reported before for polyaniline [10,12,21], however it is present in all other spectra.

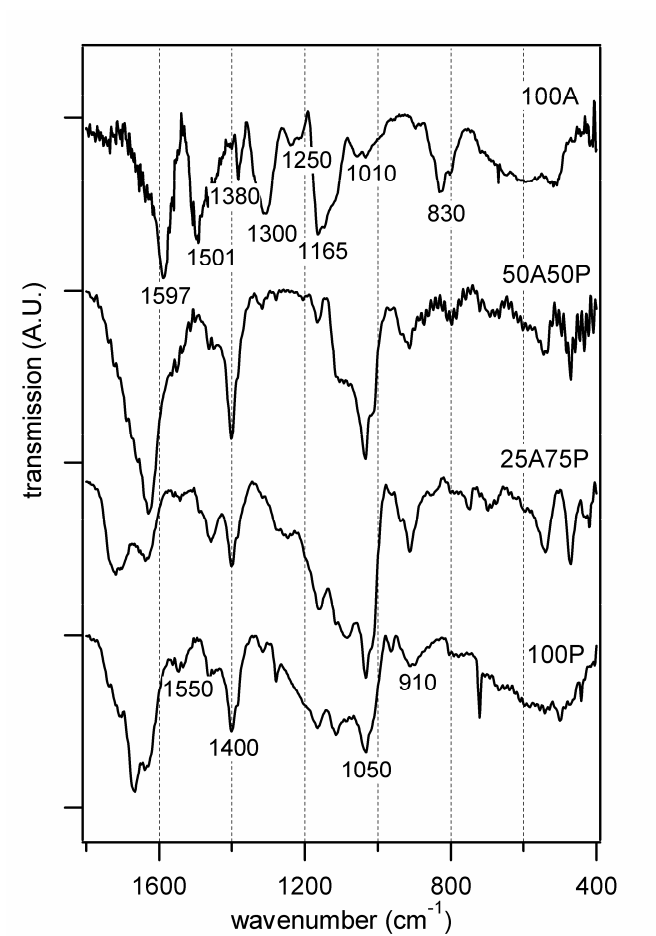


**Figure 2.** FTIR results for homopolymers and copolymers synthesized from oxalic acid without DBSA. Typical peaks for polyaniline (top) and polypyrrole (bottom) are indicated.

The FTIR spectrum taken for the polypyrrole sample deposited from the oxalic acid only electrolyte, 100P, shows typical bands at  $1550\text{ cm}^{-1}$  ( $-\text{C}=\text{N}-$ ,  $-\text{C}-\text{N}-$ ), at  $1400\text{ cm}^{-1}$  (N-H) and  $1050\text{ cm}^{-1}$  and  $910\text{ cm}^{-1}$  (characteristic vibration of the pyrrole ring) [13,23,24].

The characteristic bands for DBSA (figure 3) are  $1159\text{--}1174\text{ cm}^{-1}$  (for  $\text{SO}_3$ ),  $680\text{ cm}^{-1}$  and  $1041\text{ cm}^{-1}$  (both S=O stretch) [20,25], present in the spectra for pyrrole containing samples with DBSA. The  $1041\text{ cm}^{-1}$  band for DBSA overlaps with the  $1050\text{ cm}^{-1}$  band of polypyrrole. For polyaniline deposited from the DBSA containing electrolyte, 100As, there is no clear indication of the presence of DBSA. In this FTIR spectrum, the quinoid and benzenoid peaks appear displaced at  $1580$  and  $1480\text{ cm}^{-1}$ .

For the samples from monomer mixtures bands corresponding to polypyrrole are seen predominantly, as well as a progressive displacement of peaks in the range of  $1100$  to  $1250\text{ cm}^{-1}$  for decreasing aniline content. For 50A50P a broad band can be seen in the range of  $1570$  to  $1600\text{ cm}^{-1}$  overlapping with the large  $1630\text{ cm}^{-1}$  pyrrole band, while no peak is seen at  $1500\text{ cm}^{-1}$ , indicating the presence of aniline in its quinoid form, while the band intensity at  $1550\text{ cm}^{-1}$  corresponds to the pyrrole ring and there is a change in peak shapes and displacement in the range of  $1000$  to  $1250\text{ cm}^{-1}$ . In the

polymer of 50A50Ps, small peaks typical for polyaniline can be found, such as  $1120$  and  $1270\text{ cm}^{-1}$  and several peaks have shifted (ej.  $900$ ,  $1220\text{ cm}^{-1}$ ) compared to those found in the homopolymers. For the samples 100Ps and 25A75Ps, the characteristic polypyrrole band at  $1400\text{ cm}^{-1}$  has diminished greatly, while the peak at  $910\text{ cm}^{-1}$  shows an increase. This seems to indicate that for these samples, the presence of the DBSA ions inhibits the N-H movement, allowing increased ring vibration. The spectra for 25A75P and 25A75Ps are nearly identical to 100P and 100Ps, respectively, especially for the sample with DBSA, which shows no indication of the presence of aniline at all, indicating that the aniline content in this polymer is extremely low. The preferred deposition of pyrrole is related to its lower polymerization potential, resulting in larger pyrrole blocks compared to aniline blocks.

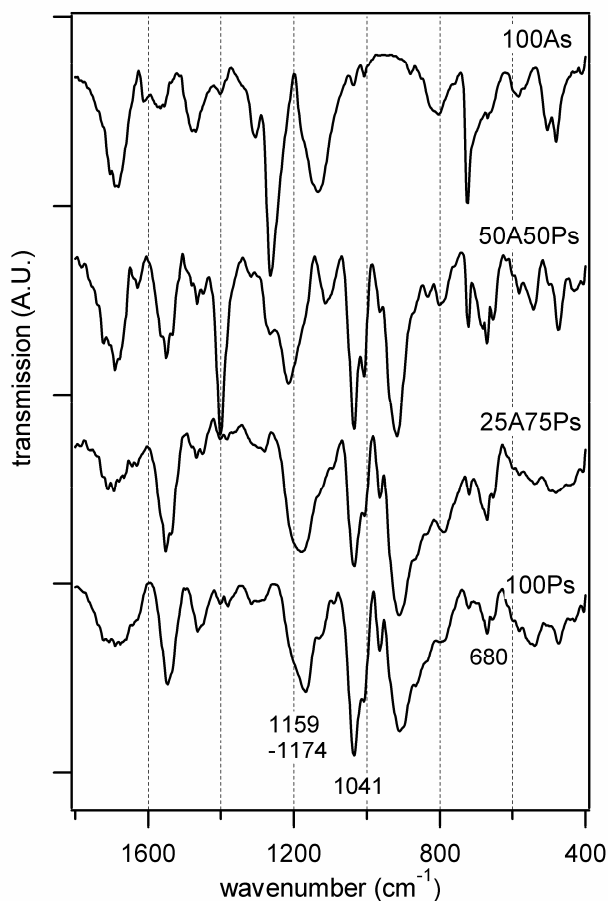


**Figure 3.** FTIR results for homopolymers and copolymers synthesized from oxalic acid and DBSA. Typical peaks for DBSA are indicated.

The spectra for the samples obtained from monomer mixtures are clearly not identical to either of the homopolymers, nor are they a superposition of the spectra of both homopolymers, as expected for mixtures [13]. The difference is caused by neighbouring aniline and pyrrole units, aniline-pyrrole heterodiads, in the polymer [13], confirming that these polymers are copolymers rather than mixtures.

### 3.3. SEM

Results of SEM micrographs for samples prepared without DBSA are shown in figure 4. The morphology of the samples is largely affected by the initial monomer composition. For 100P, a typical grain-type structure is seen, with grain diameters of 2  $\mu\text{m}$  and agglomerates with a diameter of around 10  $\mu\text{m}$  [26,27]. For 100A only a very thin layer of deposited polymer can be seen, with small grain size and a typical structure [28]. Parts of the substrate (platinum) can be seen, indicating a non-homogeneous deposition. For 75A25P hardly any polymer is present on the platinum substrate, though the grain size appears to be larger than for 100A. The micrograph for 25A75P shows that in this case more polymer was formed, though still only as a thin film, and no agglomerates can be seen.

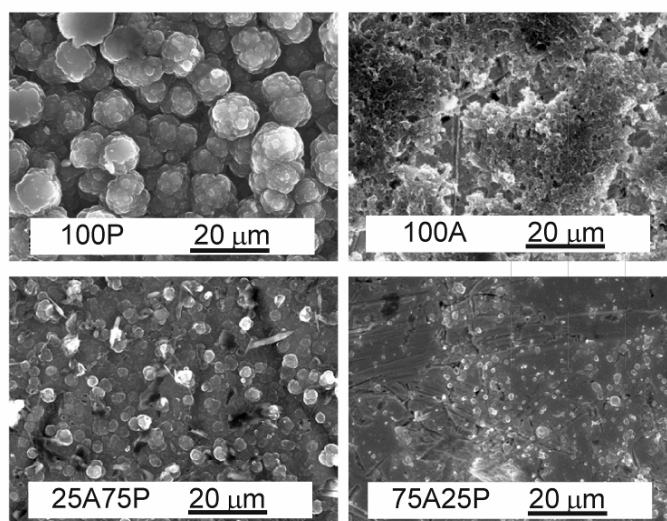


**Figure 4.** SEM micrographs for homopolymer and copolymer samples synthesized from oxalic acid without DBSA.

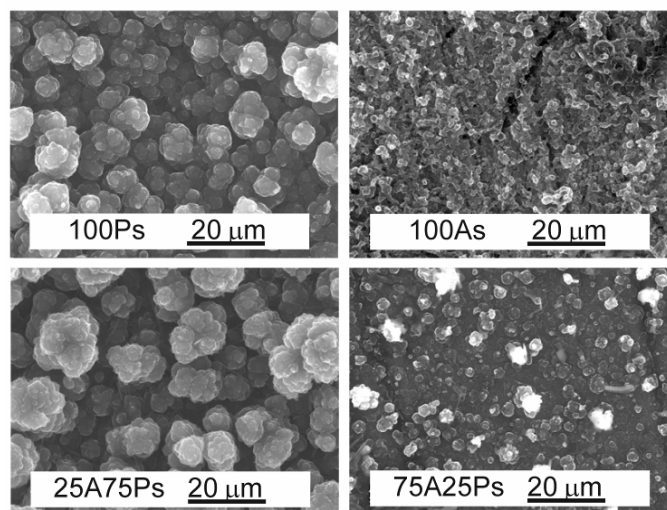


**Figure 5.** SEM micrographs for homopolymer and copolymer samples synthesized from oxalic acid and DBSA.



Figure 5 shows the SEM micrographs for samples with DBSA. In general a thicker film can be seen as compared to samples obtained without DBSA. For 100% polypyrrole, samples with and without DBSA are very similar in appearance, with similar grain size and agglomerate diameter. For 25A75Ps, a very thick film can be seen, and agglomerates have grown larger than for 100Ps. The 100As (with DBSA) film is more homogeneous than for 100A (without DBSA), with a typical grain size of 1  $\mu\text{m}$ , but without the agglomerate structure [14].

### 3.4. Cyclic Voltammetry

Results for cyclic voltammetry in a monomer-free electrolyte of 1.0 M oxalic acid are shown in figure 6. On the left hand side, results for samples without DBSA are shown. A progressive change in shape can be seen from 100% aniline towards 100% pyrrole, with increasing current densities for samples with higher pyrrole content. The large cathodic peak at -350 mV and the subsequent anodic peak at -200 mV (for 100A, 75A25P and 50A50P) are due to hydrogen evolution and proton desorption on exposed platinum substrate.

For samples with DBSA (right hand side) again a progressive change in shape with increasing current densities is found for increasing pyrrole content (with the 25A75Ps and 100Ps samples being virtually identical in shape). Peaks corresponding to hydrogen evolution and oxidation are absent, indicating complete covering of the substrate by the polymer.

For 100A the peak height and current densities diminish with progressive cycling, indicating a loss of polymer from the substrate or degradation. For 100As there is no such loss of polymer or its properties. The oxidation peak corresponding to the conversion of leucoemeraldine to emeraldine is displaced from around 200 to 400 mV. The charge associated with this conversion can be taken as a measure of the aniline content [17].

For the polypyrrole samples, current densities for samples with DBSA (100Ps) are lower than for samples without DBSA (100P), due to a lower amount of polymer formed (see table 1), however, the curve shape is very similar for both samples.

For each of the copolymers, oxidative and reductive peaks of aniline can be seen in the curves with decreasing intensity for increasing pyrrole content, confirming the presence of this monomer in the copolymer chain. The voltammogram of 25A75Ps is almost identical to that of 100Ps, confirming the result from FTIR that the aniline content in this polymer is low.

For the copolymers without DBSA bare substrate is progressively being exposed to the electrolyte and current densities for the polymer oxidation and reduction decrease with time for all 3 copolymers, as for 100A, related to a loss of polymer from the substrate. For the copolymers with DBSA, initially, rather flat curves are seen due to slow transport of the large DBSA ions, however, with time the DBSA ions are being replaced by oxalic acid ions, as can be seen from an increase in the current densities and peak heights. In none of the curves corresponding to the polymers obtained from mixed electrolyte, peaks corresponding to hydrogen reduction or desorption are observed: It is therefore concluded that deposition from the mixed electrolyte results in better adhesion of the

polymer to the substrate, as well as improved mechanical properties of the polymer films, and that these properties are not lost during this experiment.

Finally, it can be observed that all polymers and copolymers are in reduced state at PEM fuel cell anode potentials ( $-244 \text{ mV}_{\text{SCE}}$ ), while at cathode potentials (say, between  $600$  and  $800 \text{ mV}_{\text{SCE}}$ ) all are in oxidized state.

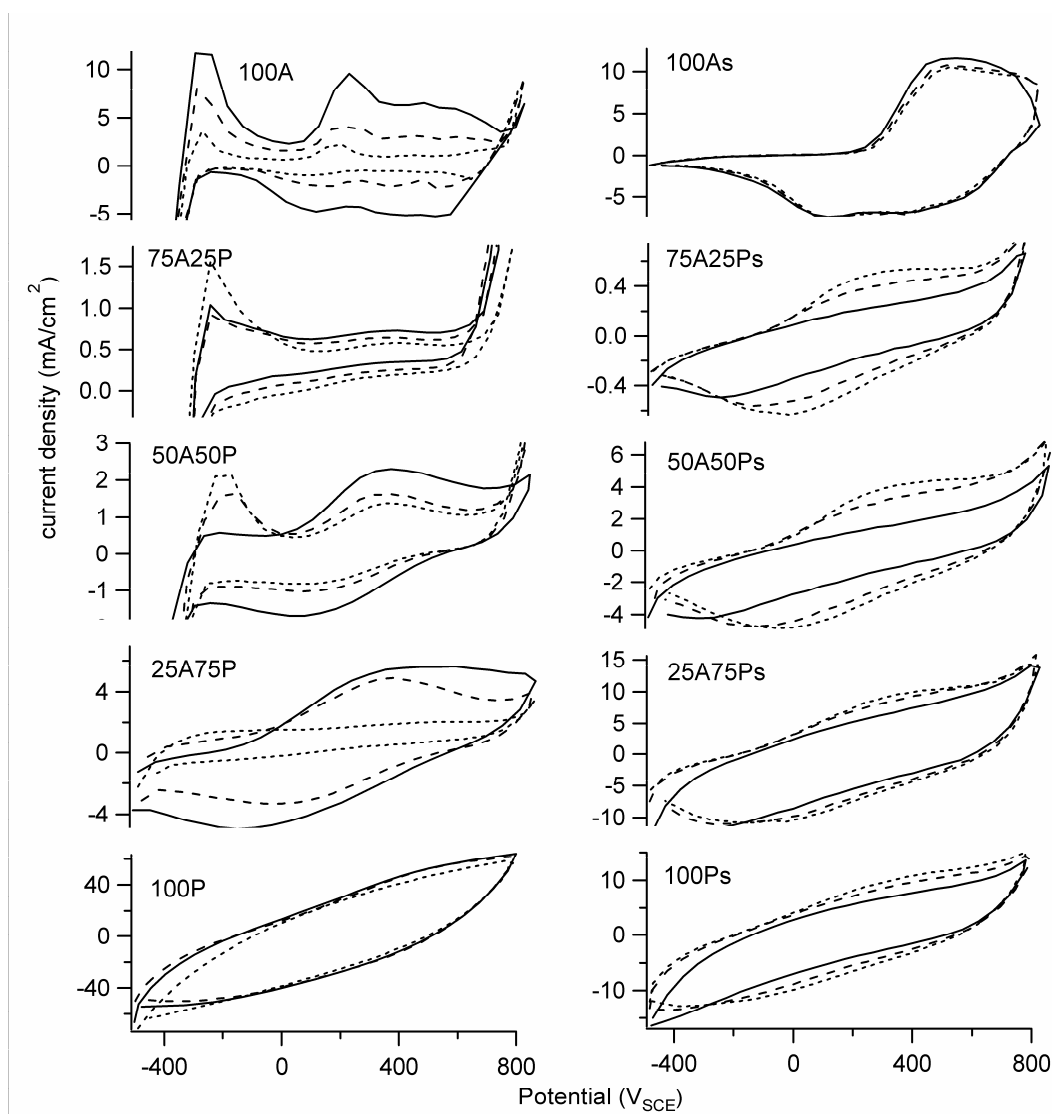


**Figure 6.** Results of cyclic voltammetry for samples in  $0.1 \text{ M}$  oxalic acid, showing first, tenth and twentieth cycle (drawn, discontinuous and dotted lines respectively). Left: polymers formed from oxalic acid only. Right: polymers with both oxalic acid and DBSA.

### 3.5. AC Impedance Spectroscopy

Figure 7 shows a series of AC impedance spectra for a sample of 50A50P. Spectra were taken once every hour during one day immersion. The high frequency semi-circle increases with time of

immersion. This behaviour of increasing impedance was found generally for all samples. The long diffusion-like tail is assumed to be due to slow dopant transport during switching-behaviour [14]. AC impedance spectra of samples after 12 hrs immersion in 0.1 M oxalic acid are shown in figures 8 and 9. The presence of DBSA results in larger impedance for the homopolymers. For the sample 75A25P, impedances were also larger in the presence of DBSA, however in this case it was related to the platinum exposed directly to the electrolyte for the sample without DBSA. For all other samples polymerized from mixed monomer solution, the presence of DBSA resulted in reduced impedance, related to the improved deposition rate of the polymer. The spectra were fitted to the equivalent circuits as shown in figure 10. For the bare platinum electrode, the circuit shown in figure 10a was used, as for 75A25P. For most samples the circuit shown in figure 10b was used, with  $R_{\Omega}$  representing the ohmic resistance of the electrolyte (and of low-conductive coatings),  $Q_{dl}$  being a CPE representing the double layer capacity (in stead of a pure capacitor),  $R_{pol}$  representing polarization resistance and  $Q_{lf}$ , a low frequency constant phase element (CPE), representing electrochemical, diffusion and switching processes [18,29]. For two samples a modified circuit had to be used, in order to be able to obtain a reasonable fit. For 100A a circuit representing two different layers had to be used (figure 10c) [30] and for 25A75P the circuit in figure 10d was used, probably related to the formation of layers or regions with different monomer composition in the polymer.

The values obtained for the different elements from fitting the equivalent circuits to the measured impedance spectra are shown in table 2. The ohmic resistance as determined for the bare platinum electrode is the resistance due to the electrolyte resistance. For the polymer samples, most samples have ohmic resistance similar to the solution resistance, indicating the relatively high conductivity of the samples. However, for the samples 75A25P and 50A50P the ohmic resistance is significantly higher, confirming the lower conductivity of these copolymers. Therefore the aniline present in these polymers is assumed to be either in the oxidized, quinoid form (as also suggested by FTIR), due to a disruption of the alternating single-double bond structure of the polymer backbone by aniline monomer isolated between pyrrole monomers. For 75A25P, the ohmic resistance is higher than the solution resistance, though not as high as for 75A25Ps, due to the direct exposure of part of the platinum substrate.

Double layer capacitance was modeled as a constant phase element and the general high values for the power  $n$ , close to 1, confirms that this element represents a capacitance. Values are highest for the homopolymers and for samples with DBSA they are of the same order or higher then for compounds without DBSA. Higher double layer capacities are related to an increased pseudocapacitance [17,31]. The polarization resistance for samples without DBSA is lowest for the homopolymers, while highest for the copolymers, with the highest value obtained for 75A25P, followed by 50A50P and 72A25Ps (those samples with highest ohmic resistance). For the samples without DBSA, values for the polarization resistance are obtained in the order of 100A < 100P < 25A75P < 50A50P < 75A25P, while for samples with DBSA the order is 100As < 50A50Ps < 25A75Ps < 100Ps < 75A25Ps. The low frequency constant phase element shows a large range of values, and is related to diffusional effects as well as to the capacity for charge storage (pseudocapacitance). Highest values are found for the homopolymers (compared to the polymers from

mixed monomer solutions) and, generally, values are higher for the polymers having DBSA included, except for 100Ps, following the same tendency as the amount of polymer formed (see table 1).

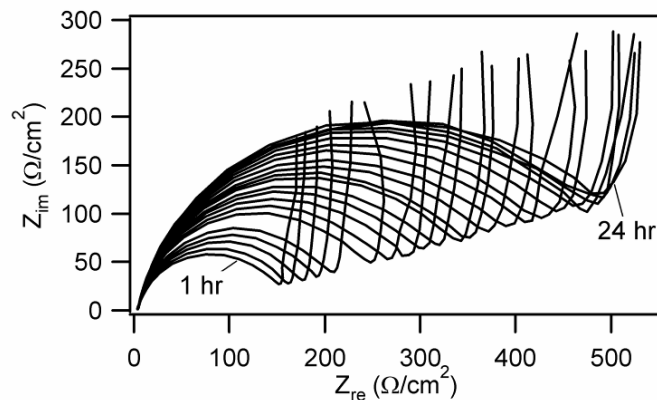


**Figure 7.** AC Impedance spectra for 50A50P in 0.1M oxalic acid, during 24 hours of immersion, with 1 hour between each measurement. Frequency range from 0.1 to 1000 Hz.

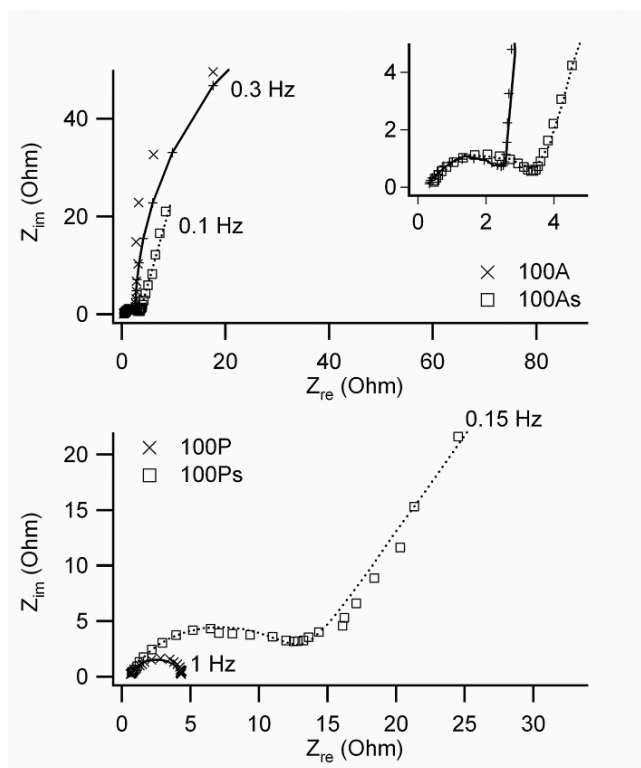


**Figure 8.** AC Impedance spectra for homopolymers polyaniline (top) and polypyrrole (bottom) at open circuit potential, after 12 hours of immersion in 0.1M oxalic acid. Applied frequencies from 0.1 to 1000 Hz.

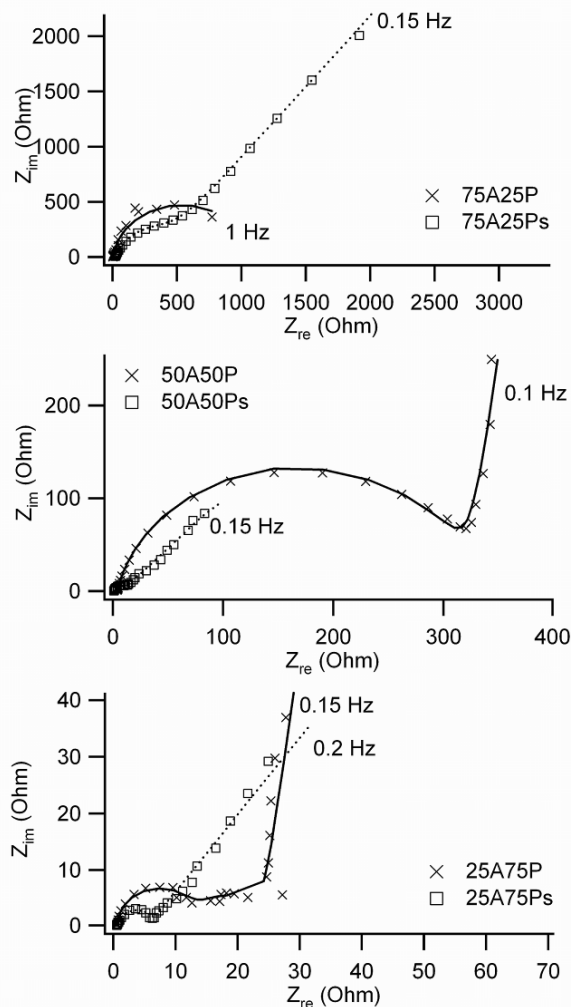


**Figure 9.** AC Impedance spectra for copolymers 50A50P and 50A50Ps (top) and 25A75P and 25A75Ps (bottom) at open circuit potential, after 12 hours of immersion in 0.1M oxalic acid. Frequencies from 0.1 to 1000 Hz.

#### 4. CONCLUSIONS

Copolymers deposited from a mixed electrolyte of oxalic acid and DBSA had higher polymerization rates, and formed thicker and more homogeneous polymer films than the corresponding copolymers deposited from oxalic acid only. For the homopolymers, deposition rates were highest when polymers were deposited without DBSA. DBSA was therefore found to improve polymerization for the copolymers only.

FTIR and cyclic voltammetry confirmed the presence of aniline in the codeposited polymers, though only in small quantities, confirming preferred deposition of pyrrole. Based on FTIR spectra it was confirmed that copolymers were formed. Cyclic voltammetry showed that samples with DBSA in an oxalic acid electrolyte show increasing current densities with time, indicating that during potential

cycling the large DBSA dopant-ion is being replaced by the smaller oxalic acid. However the improved mechanical properties were not lost.

From AC impedance spectroscopy it could be determined that the presence of DBSA results in lower impedances for those copolymers prepared with lower aniline contents (50/50% and 25/75% aniline/pyrrole respectively), due to reduced polarization resistance and improved conductivity. For co-deposited polymers with higher aniline content (75/25% aniline/pyrrole) low conductivities were found, explaining the low electrodeposition rates. Highest capacitance values (double layer and low frequency) were obtained for the homopolymers.

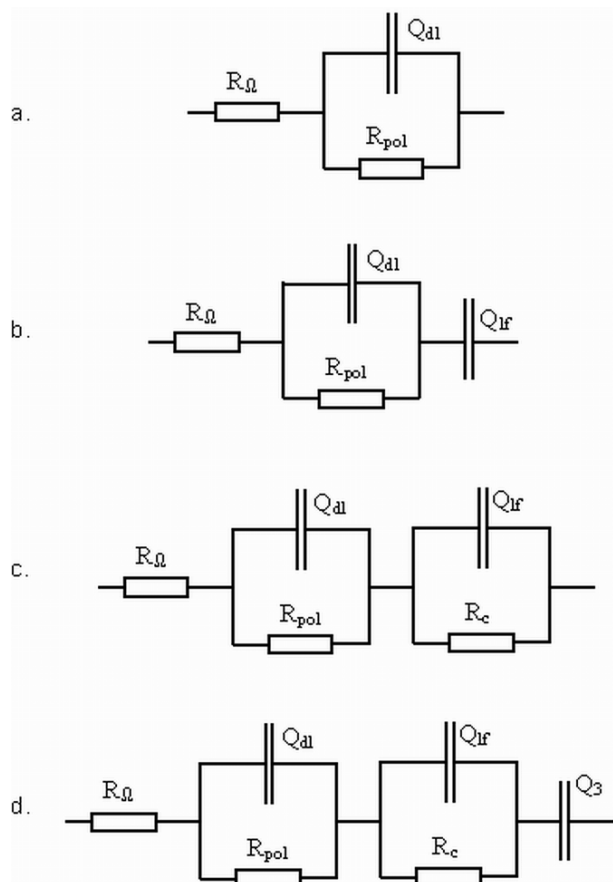


**Figure 10.** Equivalent circuits used to fit measured impedance data: a. for platinum and 75A25P; b. for 50A50P, 100P, 100As, 75A25Ps, 50A50Ps, 25A75Ps and 100Ps; c. for 100A; d. for 25A75P

#### ACKNOWLEDGEMENTS

We are grateful for the financial support given by CONACYT, project J33991-U. Furthermore, we would like to thank Dr. M.A. Espinosa-Medina and the IMP (Instituto Mexicano de Petroleo) for his help with SEM and the CIE-UNAM (Centro de Investigación en Energía) for providing their facilities during part of this research.

**Table 2.** Values obtained for the components of the equivalent circuits for AC impedance spectra at 12 hours immersion.

sample	circuit	$R_{\Omega}$ ( $\Omega$ )	$Q_{dl}$ ( $\mu\text{F}$ )	$n_{dl}$	$R_{pol}$ ( $\Omega$ )	$Q_{if}$ ( $\mu\text{F}$ )	$n_{if}$
platinum	R(RQ)	0.43	75	1	213	-	-
100A*	R(RQ)(RQ)	0.3	539	0.87	2.3	9.33E+03	1
75A25P	R(RQ)	2.1	65	0.92	1066	-	-
50°50P	R(RQ)Q	3.6	85	0.87	318	6.30E+03	0.92
25°75P**	R(RQ)(RQ)Q	0.55	65	1*	12	3.00E+03	0.83
100P	R(RQ)Q	0.61	460	0.86	3.8	2.00E+05	1
100As	R(RQ)Q	0.4	690	0.81	3	6.40E+04	0.84
75°25Ps	R(RQ)Q	17	42	0.94	295	417	0.58
50°50Ps	R(RQ)Q	0.61	76	1	7	7.80E+03	0.53
25°75Ps	R(RQ)Q	0.52	120	0.99	4.97	1.89E+04	0.6
100Ps	R(RQ)Q	0.6	566	0.77	12.1	4.30E+04	0.67

\* The value for  $R_c$  was determined to be  $158 \Omega/\text{cm}^2$ .

\*\* The value for  $R_c$  was determined to be  $11 \Omega/\text{cm}^2$ , while for  $Q_3$  and  $n_3$  values of 37 mF and 0.92 were found, respectively.

## References

1. S. Kim and S.J. Park, *Solid State Ionics*, 178 (2008) 1915
2. H. Zhao, L. Li, J. Yang and Y. Zhang, *J. Power Sources*, in press, 2008
3. R. Bashyan and P. Zeleney, *Nature*, 443 (2006) 63.
4. V. Gupta and N. Miura, *Materials Letters*, 60(2006) 1466
5. H. Mi, X. Zhang, X. Ye and S. Yang, *J. Power Sources*, 176, 403
6. S.K. Dhawan and D.C. Trivedi, *Synth. Metals*, 60(1993) 63.
7. J.A Conklin, S.-C. Huang, S.-M. Huang, T. Wen and R.B. Kaner, *Macromolecules*, 28(1995) 6522.
8. M. Lu, X.-H. Li and H.-L. Li, *Mater. Sci. Eng.*, A334(2002) 291.
9. B. Sari and M. Talu, *Synth. Metals*, 94(1998) 221.
10. F. Fusalba and D. Bélanger, *J. Phys. Chem.*, 103(1999) 9044.
11. R. Rajagopalan and J.O. Iroh, *Electrochim. Acta*, 47 (2002) 1847.
12. R. Rajagopalan and J.O. Iroh, *Appl. Surface Sci.*, 218 (2003) 58.
13. J. Stejskal, M. Trchová, I.A. Ananieva, J. Janca, J. Prokes, S. Fedorova and I. Sapurina, *Synth. Metals*, 146 (2004) 29.
14. V.W. Lim, E.T. Kang, K.G. Neoh, Z.H. Ma and K.L. Tan, *Applied Surface Science*, 181 (2001) 317.
15. M. Reghu, Y. Cao, D. Moses and A.J. Heeger, *Phys. Rev. B*, 47 (1993) 1758.
16. W. Jia, R. Tchoudakov, E. Segal, R. Joseph, M. Narkis and A. Siegmann, *Synth. Metals*, 132 (2003) 269.
17. G.W. Wallace, G.M. Spinks, L.A.P. Kane-Maguire and P.R. Teasdale, *Conductive Electroactive Polymers, Intelligent Materials Systems*, ed. CRC Press, 2003.

18. W.-C. Chen, T.-C. Wen and A. Gopalan, *Synth. Metals*, 128 (2002)179.
19. S. H. Jang, M.G. Han and S.S. Im, *Synth. Metals*, 110 (2000) 17.
20. M.G. Han, Y.J. Lee, S.W. Byun and S.S. Im, *Synth. Metals*, 124 (2001) 337.
21. J.L. Camalet, J.C. Lacroix, S. Aeiyaich, K. Chane-Ching and P.C. Lacaze, *Synth. Metals*, 93 (1998) 133.
22. P.D. Gaikwad, D.J. Shirale, P.A. Savale, K. Datta, P. Gosh, A.J. Pathan, G. Rabbani and M.D. Shirsat, *Int. J. Electrochem. Sci.*, 2 (2007) 488.
23. R. Rajagopalan and J.O. Iroh, *Electrochim. Acta*, 46 (2001) 2443.
24. J.O. Iroh and Y. Chen, *Pol. Composites*, 20 (1999) 482.
25. X. Lu, H.Y. Ng, J. Xu and C. He, *Synth. Metals*, 128 (2002)167.
26. N. Bhat, P. Geetha and S. Pawde, *Pol. Eng. Sci.*, 39 (1999) 1517.
27. J.I. Martins, T.C. Bazzaoui, E.A. Reis, E.A. Bazzaoui and L. Martins, *Synth. Metals*, 129 (2002) 221.
28. T.-C. Wen, L.-M. Huang and A. Golapan, *J. Electrochem. Soc.*, 148 (2001) D9.
29. J. Tanguy, N. Mermilliod and M. Hoclet, *J. Electrochem Soc.*, 134 (1987) 795.
30. A.S. Sarac, M. Ates and B. Kilic, *Int. J. Electrochem. Sci.*, 3 (2008) 777.
31. M.D. Levi and D. Aurbach, *J. Electrochem. Soc.*, 149 (2002) E215.